IEEE Photonics Journal
An IEEE Photonics Society Publication

Open Access

Generalized Method to Describe the Propagation of Pulses in Classical and Specialty Optical Fibers

(Invited Paper)

Volume 11, Number 5, October 2019

Andrés Macho, ***Member, IEEE***
Roberto Llorente, ***Member, IEEE***

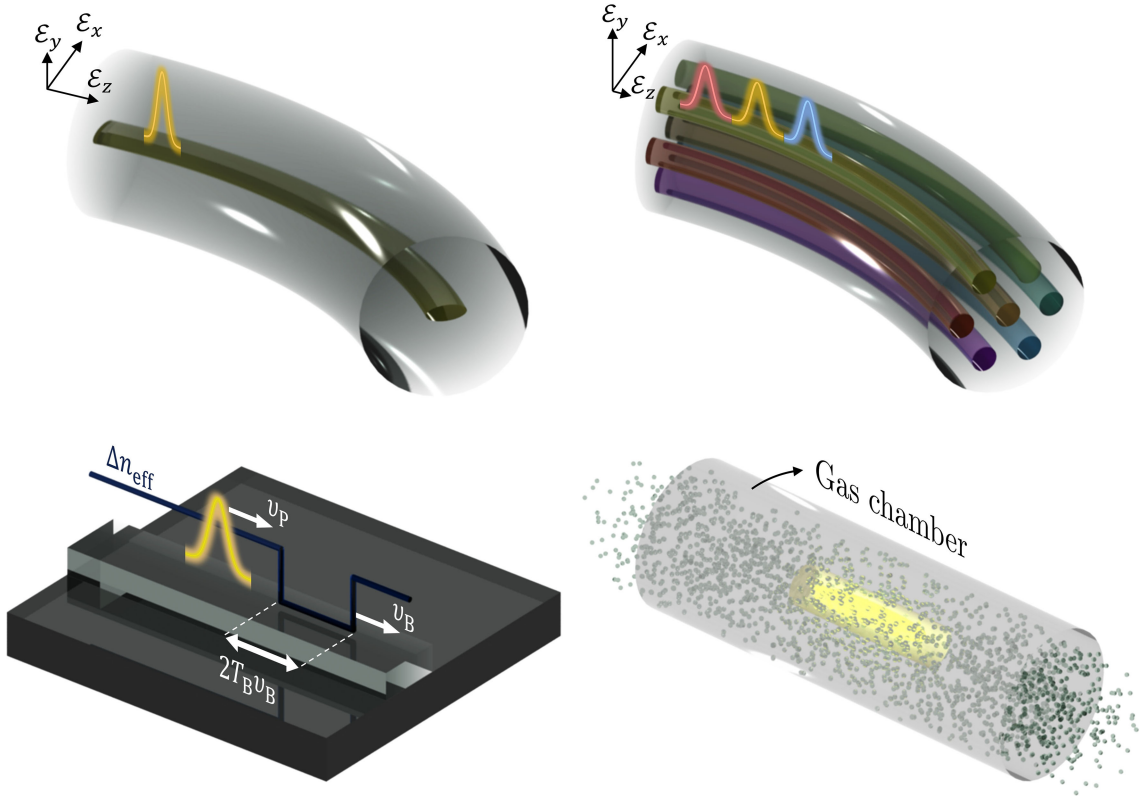

DOI: 10.1109/JPHOT.2019.2938801

IEEE photonics SOCIETY
IEEE

Generalized Method to Describe the Propagation of Pulses in Classical and Specialty Optical Fibers

(Invited Paper)

Andrés Macho, *Member, IEEE*, and Roberto Llorente, *Member, IEEE*

The authors are with the Nanophotonics Technology Center, Universitat Politècnica de València, Valencia 46022, Spain

DOI:10.1109/JPHOT.2019.2938801

Manuscript received July 30, 2019; revised August 25, 2019; accepted August 28, 2019. Date of publication September 2, 2019; date of current version September 30, 2019. This work was supported in part by the Spain National Plan project MINECO/FEDER UE RTI2018-101296-B-I00 MULTI- BEAM5G, and in part by the Generalitat Valenciana Plan project GVA AICO/2018/324 NXTIC. *(Corresponding author: Andrés Macho.)*

This paper has supplementary downloadable material available at http://ieeexplore.ieee.org, provided by the authors.

Abstract: The comprehension of pulsed light propagation is of paramount importance in fiber optics. Here, we present a general method to describe the propagation of pulses in any kind of optical fiber, regardless of its fabrication process or constituent materials. As a result, we obtain a rich toolbox for the analysis and synthesis of optical fibers, which allows us to circumvent the resolution of Maxwell's equations by using heavy-computational numerical methods. To illustrate this, we analyze the pulse propagation problem in non-paraxial anisotropic single-core and multi-core fibers that cover a large variety of optical fibers including classical weakly guiding fibers, optical gain fibers, polarization-maintaining fibers, highly nonlinear fibers, and photonic crystal fibers. Moreover, it is shown that our method can be applied to any kind of guided and unguided medium undergoing spatial and temporal perturbations, provided that the distance and temporal width between different consecutive spatial and temporal medium perturbations are respectively higher than the spatial and temporal width of the optical pulses.

Index Terms: Optical fiber, optical pulses, nonlinear optics.

1. Introduction

Since the introduction of Maxwell's equations in 1865 [1], engineers have been able to unveil a large gamut of electromagnetic technologies, among others, the optical fiber. Outstandingly, optical fiber has sparked a new paradigm in communications as it has significantly increased the Shannon capacity of our communication networks based on metallic waveguides [2]. Moreover, optical fiber technology has also uncovered new possibilities and applications in other fields of science, such as in experimental physics (e.g., to study exotic phenomena such as the Hawking radiation using analog gravity [3]) and in biomedicine (e.g., to develop crucial advances in lasers [4], sensors [5] and medical imaging [6]). In this vein, diverse types of optical fibers have been proposed and developed in the last decades: the standard single-mode fiber [7], photonic crystal fibers [8], fiber

lasers [4], polarization-maintaining fibers [9], highly-nonlinear fibers [10], and multi-core fibers [11], to name a few.

Therefore, considering the enormous potential of optical fiber technology, the comprehension of the electromagnetic wave propagation in this medium is of capital importance and, in particular, the propagation of pulsed electromagnetic waves (polychromatic waves) in order to cover as many propagation effects as possible.

A rigorous theoretical analysis of the pulse propagation problem in an optical fiber should be performed by solving Maxwell's equations. Unfortunately, in this scenario, an analytic solution of these equations is not always possible (e.g., in some gradual-index single-core fibers [12]) and, in such a case, numerical simulations are required. A variety of numerical methods to solve Maxwell's equations in an optical fiber have been reported in the literature [13]–[24].

The most accurate numerical analysis technique is the finite-difference time-domain (FDTD) method (also known as Yee's method) [13]. Despite the fact that FDTD is applicable to any kind of optical fiber, this technique requires a fine discretization of the spatial and temporal grids using respectively the scale of the wavelength and time period of the electromagnetic fields. Hence, numerical calculations of Maxwell's equations based on FDTD usually require a high computational time and memory consumption when analyzing several meters or kilometers of propagation.

An accurate numerical solution of Maxwell's equations in an optical fiber can also be explored via the eigenmode expansion (EME) method [14], [15]. This technique is generally much more efficient than FDTD as it does not demand a fine discretization of the independent variables on the scale of the wavelength and time period of the electromagnetic fields. Nevertheless, the required computational time and memory consumption may be highly increased, concretely, when fiber nonlinear effects and a high number of guided modes are involved in the pulse propagation problem. In such a case, EME should be combined with heavy-computational iterative techniques which account for the nonlinear changes of the fiber modes [16].

The natural strategy to solve numerically Maxwell's equations in the pulse propagation problem is the beam propagation method (BPM) [17], [18]. Bearing in mind that, in general, we are interested in analyzing fiber distances ranging from several meters to kilometers, it is more suitable to consider a numerical method which involves a discretization of the spatial and temporal grids by using respectively the scale of the spatial and temporal width of the optical pulses. In other words, the complexity of the numerical calculations of Maxwell's equations can be alleviated in an optical fiber if we are able to describe only the propagation of the slowly-varying longitudinal and temporal evolution of the pulsed electromagnetic waves, the so-called complex envelope [see Fig. 1(a)]. This idea leads to a system of pulse propagation equations (PPEs) which accounts for the spatio-temporal evolution of the complex envelopes associated to the electromagnetic fields propagated through the optical fiber under analysis.

An outstanding problem in the BPM literature is a general procedure which allows us to derive systematically the system of PPEs in any kind of optical fiber. The theoretical approaches reported in this topic are usually tedious and complex, especially when Maxwell's equations are combined with perturbation theory or higher-order nonlinear effects are considered [19]–[24]. Furthermore, most of these approaches usually neglect the longitudinal component of the fiber modes, which reduces the suitability of the BPM to weakly-guiding optical fibers (paraxial regime) [25], and omit the spatial and temporal medium perturbations (fiber bending, twisting, manufacturing imperfections, environmental temperature fluctuations and floor vibrations, among others [23], [26]), which restricts the simulation scenario to unrealistic conditions and, consequently, not being of application in crucial areas of optical fiber technology (e.g., in transport networks, where the fiber bending and twisting or the environmental temperature fluctuations may acquire a fundamental relevance in the transmission performance [27]–[29]).

Here, we present a general and systematic procedure, termed as the generalized pulse propagation method (GPPM), to derive a system of PPEs in any kind of optical fiber without the necessity of assuming weakly-guiding conditions and with the possibility of including the spatial and temporal medium perturbations (and therefore, allowing for the analysis of spatial and temporal scattering phenomena) in combination with higher-order nonlinear effects such as the Raman scattering

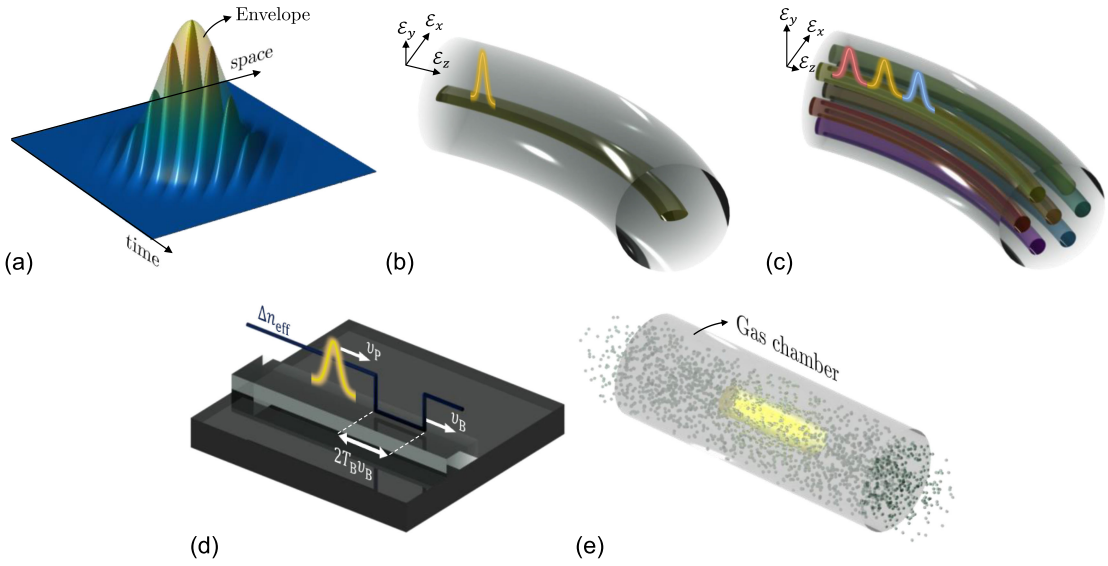

Fig. 1. Pulsed electromagnetic wave and different testbeds of the GPPM. (a) Spatio-temporal profile of a pulsed electromagnetic wave including the rapidly-varying (solid surface) and slowly-varying (semi-transparent surface) oscillations of the electromagnetic fields. Specifically, the analytic representation of the semi-transparent surface is the so-called complex envelope (the analytic representation of a function is defined in Supplementary Section 1). Along this line, it should be remarked that, in an optical waveguide, the spatial axis of reference is the longitudinal axis (z-axis), which accounts for the propagation direction of the electromagnetic energy. (b) Nonparaxial, anisotropic (highly-birefringent), single-core optical fiber propagating an ultra-short pulse in the fundamental mode modulated by a single optical carrier. (c) Paraxial, anisotropic (lowly-birefringent), multi-core optical fiber propagating different pulses modulated by different optical carriers in the fundamental mode of each core (we only represent the propagation in a given core for clarity). (d) Optical pulse propagating through a single-mode rectangular waveguide undergoing a moving temporal perturbation of the effective refractive index of the fundamental mode, encoded by the function $\Delta n_{\text{eff}}(t - z/\upsilon_{\text{B}})$. The perturbation (defined in a temporal window of width $2T_{\text{B}}$ and moving through the longitudinal axis of the optical waveguide with a speed υ_{B} lower than the group velocity of the fundamental mode υ_P) can confine optical pulses, which leads to the concept of temporal waveguide. (e) Ultra-short pulsed paraxial wave propagating through an unguided medium perturbed by an ionized gas (plasma).

(considering not only the isotropic response, but also the anisotropic response, usually omitted in the literature [17]–[24]). In this fashion, we provide a rich toolbox of analysis and synthesis of optical fiber technology circumventing the necessity of solving Maxwell's equations by using heavy-computational numerical methods. To illustrate the power of our method, we analyze the pulse propagation problem in non-paraxial (i.e., when the weakly-guiding approximation of [25] does not hold) anisotropic single-core and multi-core fibers, which covers a large variety of optical fibers including: classical weakly-guiding fibers, optical gain fibers, polarization-maintaining fibers, highly-nonlinear fibers and photonic crystal fibers [Fig. 1(b) and (c)]. Moreover, in order to further unfold the scope of our results, we demonstrate that the presented method is also applicable to any kind of guided and unguided medium undergoing spatial and temporal medium perturbations, provided that the distance (temporal width) between different consecutive spatial (temporal) perturbations is higher than the spatial (temporal) width of the optical pulses. To show this, we also analyze the pulse propagation problem in two different promising scenarios in nonlinear optics [Fig. 1(d) and (e)]: (*i*) a temporal waveguide (a moving temporal perturbation of the effective refractive index of a guided mode supported by an optical waveguide, e.g., a rectangular waveguide) and (*ii*) an unguided medium perturbed by an ionized gas (a basic platform for white-light continuum generation [30]). In the following, we will describe the different steps of the method and, next, we will delve into the different cases of study.

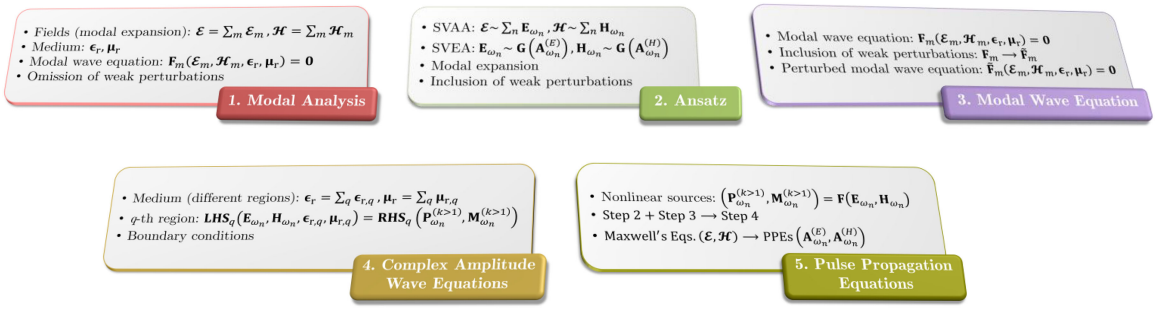

Fig. 2. Schematic description of the different steps which compose the GPPM. The slowly-varying spatial and temporal oscillations of the electromagnetic fields $\mathcal{E}$ and $\mathcal{H}$, encoded by the so-called complex envelopes $\mathbf{A}_{\omega_n}^{(E)}$ and $\mathbf{A}_{\omega_n}^{(H)}$, are extracted from Maxwell's equations by using the SVAA and the SVEA. As a result, a system of PPEs accounting for the forward and backward propagation of the complex envelopes is obtained by considering the spatial and temporal medium perturbations.

2. Results

Fig. 2 illustrates the different steps which compose the GPPM, which must deal with the description of the different frequencies (wavelengths) associated to the slowly-varying oscillations of the pulsed electromagnetic wave propagating through the analyzed medium. This can be done in a simple and elegant fashion in the different steps of the proposed method working in ω-space (**k**-space) by applying the temporal (spatial) Fourier transform to the electromagnetic fields involved in the optical propagation. Nonetheless, it should be noted that such transformations are not necessary operations in the GPPM given that are only mathematical tools that facilitate the applicability of the method in perturbed and unperturbed media.

In particular, in absence of medium perturbations or in presence of homogeneous time-invariant perturbations, we can use the classical temporal (spatial) Fourier transform. For instance, this is the case in our example presented in Section 2.4, which corresponds with the medium illustrated in Fig. 1(e). Otherwise, in presence of heterogeneous or time-varying perturbations, the classical temporal (spatial) Fourier transform is not able to describe the time-varying (heterogeneous) nature of the medium perturbations in ω-space (**k**-space). In such circumstances, we can use the short-time (short-space) Fourier transform to retain the temporal (spatial) nature of the medium perturbations in the frequency (wavenumber) domain. As an example, this is the case in the scenarios analyzed in Sections 2.1, 2.2 and 2.3, depicted in Fig. 1(b)–(d), respectively. In Supplementary Section 1, we include a detailed description of these transformations along with some basic notes about the formalism and notation employed in the GPPM.

Step 1 (modal analysis): In this step, we should perform a modal analysis of the desired medium by omitting the weak perturbations of the medium. A medium perturbation is said to be of weak nature if, by definition, the fluctuation generated in the magnitude of the effective refractive index of the pulse is much lower than its magnitude in absence of such a perturbation. In guided media, the effective refractive index of the pulse is the same as that of the guided mode over which the pulse propagates. In unguided media, the effective refractive index of the pulse is the material refractive index of the medium.

For instance, in an optical fiber, we can observe medium perturbations of weak nature such as: losses, nonlinear effects, fiber bending, fiber twisting, manufacturing imperfections, environmental temperature fluctuations, and floor vibrations. In general, this is the case of any kind of optical fiber, also including highly-nonlinear optical fibers [10] and optical gain fibers, where amplification can be regarded as a negative absorption (negative losses) [4]. Hence, in the case of optical fibers, the modal analysis should be performed in the linear regime and omitting the fiber losses and the additional medium perturbations.

Step 2 (ansatz): Here, our goal is to propose the ansatz of the real representation of the electric and magnetic field strengths ($\mathcal{E}$ and $\mathcal{H}$) by including heuristically the weak perturbations of the

medium in the results of step 1 (however, in this step, we can omit the nonlinear effects to reduce the computational time of the final system of PPEs, provided that the medium has a weak nonlinear nature). Likewise, the ansatz of $\mathcal{E}$ and $\mathcal{H}$ must also describe both forward and backward propagations. Backward propagation is usually omitted in the literature [17]–[24], but is crucial to perform a complete description of the spatial and temporal scattering problems (see below step 4).

Moreover, we must decouple the rapidly- and slowly-varying temporal and spatial changes of the ansatz by using the slowly-varying amplitude (SVAA) and envelope approximations (SVEA), respectively. The SVAA requires to write the analytic representation of $\mathcal{E}$ and $\mathcal{H}$ as a function of the complex amplitudes $\mathbf{E}_{\omega_n}$ and $\mathbf{H}_{\omega_n}$, where $\{\omega_n\}_{n=1}^{N}$ is the set of angular frequencies associated to the optical carriers of the problem, which can be generated by an external source [e.g., different lasers in a wavelength-division multiplexing (WDM) system] or by nonlinear effects of the medium (e.g., four-wave mixing). Specifically, $\mathcal{E}$ and $\mathcal{H}$ can be written by using the SVAA as follows:

$$\mathcal{E}(\mathbf{r}, t) = \mathrm{Re}\{\mathbf{E}(\mathbf{r}, t)\} \simeq \sum_{n=1}^{N} \mathrm{Re}\left\{\mathbf{E}_{\omega_n}(\mathbf{r}, t)\exp(\mathrm{j}\omega_n t)\right\}; \tag{1}$$

$$\mathcal{H}(\mathbf{r}, t) = \mathrm{Re}\{\mathbf{H}(\mathbf{r}, t)\} \simeq \sum_{n=1}^{N} \mathrm{Re}\left\{\mathbf{H}_{\omega_n}(\mathbf{r}, t)\exp(\mathrm{j}\omega_n t)\right\}, \tag{2}$$

assuming that $\|\delta_t \mathbf{E}_{\omega_n}\| \ll \|\mathbf{E}_{\omega_n}\|$ in $\delta t \sim 2\pi/\omega_n$, where $\delta_t \mathbf{E}_{\omega_n}(\mathbf{r}, t) := \mathbf{E}_{\omega_n}(\mathbf{r}, t) - \mathbf{E}_{\omega_n}(\mathbf{r}, t + \delta t)$ (the same premise applies to $\mathbf{H}_{\omega_n}$). In particular, the SVAA allows us to decouple the rapid temporal oscillation of the optical carriers from the slow temporal evolution of the optical pulses, encoded by $\mathbf{E}_{\omega_n}$ and $\mathbf{H}_{\omega_n}$. Therefore, the method proposed herein is valid if and only if Maxwell's equations are approximately satisfied when using Eqs. (1) and (2). However, this assumption is not fulfilled if the pulses are too narrow, namely around the order of the period of the optical carriers or shorter [31]. In such a case, the decomposition performed in the above equations is no longer useful and the concept of the complex amplitude itself becomes unclear.

The SVEA requires to write $\mathbf{E}_{\omega_n}$ and $\mathbf{H}_{\omega_n}$ as a function of the complex envelopes $\mathbf{A}_{\omega_n}^{(E)}$ and $\mathbf{A}_{\omega_n}^{(H)}$ to decouple the rapid spatial oscillation of the optical carriers from the slow spatial evolution of the optical pulses. In complete analogy with the SVAA, the basic idea of the SVEA is to extract the rapid oscillations $\exp(\mp\mathrm{j}\mathbf{k}_n \cdot \mathbf{r})$ from the complex amplitudes of the form:

$$\mathbf{E}_{\omega_n}(\mathbf{r}, t) \sim \mathbf{A}_{\omega_n}^{(E)}(\mathbf{r}, t)\exp(\mp\mathrm{j}\mathbf{k}_n \cdot \mathbf{r}); \tag{3}$$

$$\mathbf{H}_{\omega_n}(\mathbf{r}, t) \sim \mathbf{A}_{\omega_n}^{(H)}(\mathbf{r}, t)\exp(\mp\mathrm{j}\mathbf{k}_n \cdot \mathbf{r}), \tag{4}$$

assuming that $\|\delta_{\mathbf{r}} \mathbf{A}_{\omega_n}^{(E,H)}\| \ll \|\mathbf{A}_{\omega_n}^{(E,H)}\|$ in $\|\delta\mathbf{r}\| \sim \lambda_n = 2\pi/\|\mathbf{k}_n\|$, where $\mathbf{k}_n := \mathbf{k}(\omega_n)$ is the wave vector of the n-th optical carrier, $\delta_{\mathbf{r}} \mathbf{A}_{\omega_n}^{(E,H)}(\mathbf{r}, t) := \mathbf{A}_{\omega_n}^{(E,H)}(\mathbf{r}, t) - \mathbf{A}_{\omega_n}^{(E,H)}(\mathbf{r} + \delta\mathbf{r}, t)$, and the sign – (+) accounts for the forward (backward) propagation in both equations. Interestingly, Eqs. (3) and (4) are general expressions which describe the role of the SVEA in both guided and unguided scenarios. However, these equations are found to be incomplete in guided media. In this scenario, we must also include the transverse eigenfunctions (F) of the guided modes supported by the waveguide (calculated in step 1) and perform a modal expansion of $\mathbf{E}_{\omega_n}$ and $\mathbf{H}_{\omega_n}$. In multi-core waveguides with a core-to-core distance higher than $\max\{\lambda_n\}_{n=1}^{N}$, this modal expansion can be performed by using perturbation theory: both complex amplitudes can be approximated from a linear combination of the exact modal solution of each isolated core, that is, assuming that each core is uncoupled from adjacent cores. Nonetheless, in multi-core waveguides with a core-to-core distance of the same order of magnitude as $\max\{\lambda_n\}_{n=1}^{N}$ (or lower), where perturbation theory does not hold [32], the modal expansion of $\mathbf{E}_{\omega_n}$ and $\mathbf{H}_{\omega_n}$ should be performed by using the exact supermodes of the waveguide (calculated in step 1).

In addition, it is worthy to note that the GPPM does not require to use additional approximations. This inherently implies that, in contrast with the main works on BPMs which can be found in the literature [17]–[24], the paraxial approximation is not required by our method.

Step 3 (modal wave equation): In this step, we must write the wave equation of the modes employed in step 2 to perform the modal expansion of $\mathbf{E}_{\omega_n}$ and $\mathbf{H}_{\omega_n}$. In absence of weak perturbations in the optical medium, this equation is directly known from step 1. Otherwise, the modal wave equation of step 1 should be heuristically modified to guarantee that the ansatz proposed in step 2, which includes the weak perturbations of the medium, fulfills Maxwell's equations.

Step 4 (complex amplitude wave equations): In step 4, the goal is to derive the wave equations for the complex amplitudes $\mathbf{E}_{\omega_n}$ and $\mathbf{H}_{\omega_n}$ by considering, if this is the case, the nonlinear nature of the optical medium. At the left-hand side (LHS) of the complex amplitude wave equations (CAWEs) should be written the linear terms and at the right-hand side (RHS) should be included the nonlinear sources: the complex amplitude of the nonlinear polarization (magnetization) in all-dielectric (all-magnetic) media.

Furthermore, we should also include boundary conditions to the CAWEs when there is a spatial or temporal scattering problem. Specifically, the spatial (temporal) scattering problem refers to the generation of a reflected and a transmitted wave as a result of the interaction of an incident wave with a localized spatial (temporal) variation of the constitutive parameters, the electric permittivity and magnetic permeability, through the propagation direction of the electromagnetic energy [31], [33]. In such a scenario, we should proceed in the following way:

- The problem should be separated in different spatio-temporal regions where the constitutive parameters present a slowly-varying longitudinal and temporal evolution in comparison with the longitudinal and temporal width of the optical pulses (in Supplementary Section 1 we include a rigorous definition about the concept of rapidly- and slowly-varying functions). This guarantees that reflections can be neglected in each isolated region, that is, when the propagation of each region is analyzed in uncoupled conditions from the others.
- A different set of CAWEs for $\mathbf{E}_{\omega_n}$ and $\mathbf{H}_{\omega_n}$ should be derived from Maxwell's equations for each region of the problem.
- The regions should be connected by the corresponding boundary conditions of the spatial and temporal scattering problems. The boundary conditions of the spatial scattering are the spatial continuity of the tangential component of $\mathcal{E}$ and $\mathcal{H}$ at the spatial interfaces of the problem [31]. The boundary conditions of the temporal scattering are the temporal continuity of $\mathcal{D}$ and $\mathcal{B}$ at the temporal interfaces of the problem [33].

Step 5 (pulse propagation equations): Firstly, we must calculate the nonlinear sources of the CAWEs as a function of $\mathbf{E}_{\omega_n}$ and $\mathbf{H}_{\omega_n}$. Secondly, we must substitute our ansatz (step 2) in the CAWEs (step 4) by using the modal wave equation (step 3) to simplify the algebraic work. Thirdly, we will find that the resulting equations depend on the complex envelopes $\mathbf{A}_{\omega_n}^{(E)}$ and $\mathbf{A}_{\omega_n}^{(H)}$. These equations are the sought system of PPEs. Finally, in waveguides, in order to remove the nodes (i.e., zeros) of the transverse eigenfunctions F from the PPEs, we must first multiply these equations by F^* and, later, integrate them in an infinite transverse section orthogonal to the propagation direction. A series of mode-coupling coefficients (MCCs) emerge from this integration operation, which are described by linear operators in the time domain when analyzing optical pulses in the femtosecond regime (see Section 2.1).

It should be noted that a system of PPEs is required to describe the propagation of $\mathbf{A}_{\omega_n}^{(E)}$ and $\mathbf{A}_{\omega_n}^{(H)}$ in each region of the problem (remember that, in step 4, we separated the problem in different spatio-temporal regions). Each PPE governs the propagation of a single component of $\mathbf{A}_{\omega_n}^{(E)}$ or $\mathbf{A}_{\omega_n}^{(H)}$ (6 components in total). Thus, considering both forward and backward propagations, N different optical carriers and M guided modes ($M = 1$ in unguided media), we will find a system of $6 \times 2 \times N \times M$ PPEs in each region of the problem. Nonetheless, if $\mathbf{E}_{\omega_n}$ is completely uncoupled from $\mathbf{H}_{\omega_n}$ in the CAWEs, $\mathbf{A}_{\omega_n}^{(H)}$ ($\mathbf{A}_{\omega_n}^{(E)}$) can be directly calculated from $\mathbf{A}_{\omega_n}^{(E)}$ ($\mathbf{A}_{\omega_n}^{(H)}$) by using Faraday's (Ampère's) law. In such a case, we only require a system of $3 \times 2 \times N \times M$ PPEs in each region. Finally, in order to perform a complete description of the pulse propagation problem through the whole optical medium, the boundary conditions detailed in step 4 must be included to connect the different systems of PPEs.

Once we solve numerically the different systems of PPEs, we will be able to calculate the electromagnetic power which propagates in the n-th optical carrier through the longitudinal direction $\pm\hat{u}_{\mathrm{L}}$ at a given point with vector position $\mathbf{r} = r_{\mathrm{L}}\hat{u}_{\mathrm{L}}$:

$$P_{\omega_n}(r_{\mathrm{L}}, t) = \int_{\infty} \frac{1}{2}\mathrm{Re}\left[\mathbf{E}_{\omega_n}(\mathbf{r}, t) \times \mathbf{H}^{*}_{\omega_n}(\mathbf{r}, t)\right] \cdot (\pm\hat{u}_{\mathrm{L}})\, \mathrm{d}^2 r_{\mathrm{T}}, \tag{5}$$

with the sign $+$ $(-)$ for the forward (backward) propagation and $\mathrm{d}^2 r_{\mathrm{T}}$ accounting for the differential surface of an infinite transverse section orthogonal to $\hat{u}_{\mathrm{L}}$. In the next subsections, we apply the GPPM in different optical media, sketched in Fig. 1.

2.1 Non-Paraxial Anisotropic Single-Core Fiber

As a first example that allows us to demonstrate the power of the GPPM, we tackle the pulse propagation problem in an all-dielectric (e.g., silica), lossy, nonlinear, anisotropic, non-paraxial, single-core fiber [Fig. 1(b)]. It is worth mentioning that these are general considerations which guarantee that the PPEs associated to this kind optical fiber may describe the propagation of pulses in a large gamut of single-core fibers: classical weakly-guiding fibers, optical gain fibers (amplification can be regarded as negative absorption, as mentioned before), polarization-maintaining fibers, highly-nonlinear fibers and photonic crystal fibers. In addition, all-magnetic fibers [34], [35] can also be described by the same PPEs as those of the all-dielectric case (see page 14 of Supplementary Material).

In order to describe a realistic fiber propagation, let us assume the medium perturbations detailed in the description of step 1, all of them of weak nature. In such a scenario, we will consider an ultra-short pulse (femtosecond regime) which propagates exclusively in the fundamental mode (single-mode regime) of the aforementioned fiber modulated by a single optical carrier of frequency $\omega_0/(2\pi) \sim 190$ THz.

Following the different steps of the GPPM (working in ω-space), the pulse propagation problem is described by a system of 3 PPEs which account for the forward propagation of the three components of $\mathbf{A}^{(E)}_{\omega_0}(z, t) = \sum_{i=x,y,z} \mathcal{A}_i(z, t)\hat{u}_i$ from $z = 0$ to $z = L$, where L is the fiber length. Concretely, the PPE associated to $\mathcal{A}_x$ is found to be (see Supplementary Section 2):

$$\begin{aligned}
\mathrm{j}\left(\partial_z + \hat{\mathrm{D}}^{(\mathrm{eq})}_x(z, t) + \frac{1}{2}\hat{\alpha}\right)\mathcal{A}_x(z, t) &= \hat{\mathrm{q}}^{(\mathrm{I})}_x(z, t)\left[|\mathcal{A}_x(z, t)|^2 \mathcal{A}_x(z, t)\right] \\
&+ \hat{\mathrm{q}}^{(\mathrm{R})}_x(z, t)\left[\left(f(t) * |\mathcal{A}_x(z, t)|^2\right)\mathcal{A}_x(z, t)\right] \\
&+ \sum_{i=y,z}\left\{\hat{\mathrm{M}}^{(\mathrm{eq})}_{x,i}(z, t)\,\mathcal{A}_i(z, t) + \frac{2}{3}\hat{\mathrm{g}}^{(\mathrm{I})}_{x,i}(z, t)\left[|\mathcal{A}_i(z, t)|^2 \mathcal{A}_x(z, t)\right]\right. \\
&+ \frac{1}{3}\exp\left(-\mathrm{j}2\Delta\phi^{(0)}_{i,x}(z, t)\right)\hat{\mathrm{g}}^{(\mathrm{I})}_{x,i}(z, t)\left[\mathcal{A}^{*}_x(z, t)\,\mathcal{A}^{2}_i(z, t)\right] \\
&+ \hat{\mathrm{g}}^{(\mathrm{R})}_{x,i}(z, t)\left[\left(h(t) * |\mathcal{A}_i(z, t)|^2\right)\mathcal{A}_x(z, t)\right] \\
&+ \frac{1}{2}\hat{\mathrm{g}}^{(\mathrm{R})}_{x,i}(z, t)\left\{\left[u(t) * \left(\mathcal{A}_x(z, t)\,\mathcal{A}^{*}_i(z, t)\right)\right]\mathcal{A}_i(z, t)\right\} \\
&\left.+ \frac{1}{2}\exp\left(-\mathrm{j}2\Delta\phi^{(0)}_{i,x}(z, t)\right)\hat{\mathrm{g}}^{(\mathrm{R})}_{x,i}(z, t)\left\{\left[u(t) * \left(\mathcal{A}^{*}_x(z, t)\,\mathcal{A}_i(z, t)\right)\right]\mathcal{A}_i(z, t)\right\}\right\},
\end{aligned} \tag{6}$$

with space- and time-varying linear operators accounting for the spatial and temporal medium perturbations along with the optical dispersion induced by different propagation phenomena: chromatic dispersion ($\hat{\mathrm{D}}^{(\mathrm{eq})}_x$), optical attenuation or amplification ($\hat{\alpha}$), linear intra-core mode-coupling ($\hat{\mathrm{M}}^{(\mathrm{eq})}_{x,i}$) and nonlinear intra-core mode-coupling ($\hat{\mathrm{q}}^{(\mathrm{I})}_x$, $\hat{\mathrm{q}}^{(\mathrm{R})}_x$, $\hat{\mathrm{g}}^{(\mathrm{I})}_{x,i}$, $\hat{\mathrm{g}}^{(\mathrm{R})}_{x,i}$). The nonlinear effects include the isotropic ($\hat{\mathrm{q}}^{(\mathrm{I})}_x$, $\hat{\mathrm{q}}^{(\mathrm{R})}_x$) and anisotropic ($\hat{\mathrm{g}}^{(\mathrm{I})}_{x,i}$, $\hat{\mathrm{g}}^{(\mathrm{R})}_{x,i}$) response of the nonlinear polarization associated to the

electronic ($\hat{q}_x^{(I)}$, $\hat{g}_{x,i}^{(I)}$) and nuclear ($\hat{q}_x^{(R)}$, $\hat{g}_{x,i}^{(R)}$) motions of silica atoms when an incident electromagnetic field stimulates the fiber. Specifically, Raman scattering (whose response is modeled by the *f*, *h* and *u* functions) is a well-known effect arising from the nuclear contribution to the nonlinear polarization [36]. A more detailed description about the different terms which appear in Eq. (6) can be found in Supplementary Section 2.

A complete characterization of the pulse propagation problem also requires to describe the propagation of $\mathbf{A}_{\omega_0}^{(H)}$, which can be directly calculated from $\mathbf{A}_{\omega_0}^{(E)}$ by using Faraday's law working in ω-space, as commented above in step 5. Hence, in this case, we only require a system of 3 coupled PPEs which govern the propagation of the three components of $\mathbf{A}_{\omega_0}^{(E)}$. Along this line, note that it is not required to include boundary conditions to the system of PPEs, provided that the fiber perturbations exhibit a slowly-varying nature in comparison with the longitudinal and temporal width of the optical pulses. In such circumstances, according to step 4, the pulse propagation problem can be exclusively described with the forward propagation using a unique spatio-temporal region $(z, t) \in [0, L] \times \bar{\mathbb{R}}$. This point should be revisited, for instance, in presence of rapidly-varying nonlinear refractive index changes inducing pulse reflection [37], which leads to the concept of temporal waveguide (see Section 2.3).

2.2 Multi-Core Fibers and WDM Systems

Despite the potential of the previous example, this relies on the propagation of optical pulses modulated by a single optical carrier. Nonetheless, the GPPM also allows us to describe the propagation of pulses when several optical carriers are involved in a fiber transmission. As an illustrative example, we will use the GPPM to describe the propagation of pulses in a WDM system based on multi-core fiber (MCF) [Fig. 1(c)].

Consider now an *N*-core weakly-guiding MCF operating in the single-mode regime. In each core of the fiber, the fundamental mode propagates *Q* different optical pulses wider than 10 ps and each one modulated by a different optical carrier with angular frequency $\omega_q \in \{\omega_1, \ldots, \omega_Q\}$. Furthermore, we will consider the same fiber perturbations as those of the previous example. Using the GPPM (working in ω-space), this scenario is described by a system of $2 \times Q \times N$ PPEs which must be solved using a unique spatio-temporal region $(z, t) \in [0, L] \times \bar{\mathbb{R}}$, provided that the medium perturbations can be regarded as slowly-varying perturbations in comparison with the longitudinal and temporal width of the optical pulses. Each PPE describes the forward propagation of a given component of $\mathbf{A}_{n,\omega_q}^{(E)}(z, t) \simeq \sum_{i=x,y} \mathcal{A}_{niq}(z, t)\hat{u}_i$, the complex envelope associated to the electric field strength of the fundamental mode of core *n* in the *q*-th channel of the WDM system. Specifically, the PPE associated to $\mathcal{A}_{nxq}$ is of the form (see Supplementary Section 3):

$$
\begin{aligned}
\mathrm{j}\left(\partial_z + \hat{\mathrm{D}}_{nxq}^{(\mathrm{eq})}(z, t) + \frac{1}{2}\alpha_q\right)\mathcal{A}_{nxq}(z, t) &= \mathfrak{m}_{nxq,nyq}(z, t)\exp\left(-\mathrm{j}\Delta\phi_{nyq,nxq}(z, t)\right)\mathcal{A}_{nyq}(z, t) \\
&+ \sum_{\substack{m=1 \\ m\neq n}}^{N} \kappa_{nxq,mxq}(z, t)\exp\left(-\mathrm{j}\Delta\phi_{mxq,nxq}(z, t)\right)\mathcal{A}_{mxq}(z, t) \\
&+ \sum_{r,s,p}^{R_q} q_{nxq,rsp}(z, t)\,\mathcal{A}_{nxr}(z, t)\,\mathcal{A}_{nxs}(z, t)\,\mathcal{A}_{nxp}^{*}(z, t)\exp\left(-\mathrm{j}\Delta\phi_{nrsp}^{(xxx)}(z, t)\right) \\
&+ \frac{2}{3} g_{nxq,rsp}(z, t)\,\mathcal{A}_{nxr}(z, t)\,\mathcal{A}_{nys}(z, t)\,\mathcal{A}_{nyp}^{*}(z, t)\exp\left(-\mathrm{j}\Delta\phi_{nrsp}^{(xyy)}(z, t)\right) \\
&+ \frac{1}{3} g_{nxq,rsp}(z, t)\,\mathcal{A}_{nys}(z, t)\,\mathcal{A}_{nyp}(z, t)\,\mathcal{A}_{nxr}^{*}(z, t)\exp\left(-\mathrm{j}\Delta\phi_{nrsp}^{(yyx)}(z, t)\right), \qquad (7)
\end{aligned}
$$

with space- and time-varying MCCs (instead of linear operators when operating in the picosecond regime) accounting for the spatial and temporal medium perturbations along with the optical disper-

sion induced by different propagation phenomena: chromatic dispersion ($\hat{\mathrm{D}}^{(\mathrm{eq})}_{nxq}$), optical attenuation or amplification (α_q), linear intra-core mode-coupling ($\mathfrak{m}_{nxq,nyq}$), linear inter-core mode-coupling ($\kappa_{nxq,mxq}$), and nonlinear intra-core mode-coupling ($q_{nxq,rsp}$, $g_{nxq,rsp}$). Here, the nonlinear effects include only the isotropic ($q_{nxq,rsp}$) and anisotropic ($g_{nxq,rsp}$) response of the nonlinear polarization associated to the electronic motions of silica atoms. The nuclei motions (Raman effect) can be omitted for optical pulses wider than 10 ps [36]. In Supplementary Section 3, we include a more detailed discussion about this scenario and the terms appearing in Eq. (7). Finally, note that the complex envelopes $\mathbf{A}^{(H)}_{n,\omega_q}$ can be calculated from $\mathbf{A}^{(E)}_{n,\omega_q}$ by using Faraday's law.

2.3 Temporal Waveguide

In the next example, we apply the GPPM in an optical waveguide undergoing rapidly-varying perturbations. In particular, let us consider an all-dielectric weakly-guiding rectangular waveguide operating in the single-mode regime with a non-complex, weak, rapidly-varying, temporal perturbation $\Delta n_{\mathrm{eff}}(t)$ of the effective refractive index n_{eff} of the fundamental mode. The temporal perturbation is defined in a temporal window of width $2T_{\mathrm{B}}$ and is moving through the longitudinal axis of the waveguide with a speed υ_{B} lower than the group velocity of the fundamental mode [Fig. 1(d)].

In such a scenario, we are interested in the characterization of the pulse propagation problem by assuming an optical pulse with temporal width $T_{\mathrm{P}} \in (1\ \mathrm{ps}, 2T_{\mathrm{B}})$ which propagates in the fundamental mode and is modulated by an optical carrier with frequency $\omega_0/(2\pi)$ located far from the resonant frequencies of the medium. Bearing in mind the rapidly-varying nature of the modal perturbation, we observe three different spatio-temporal regions in the problem: (*i*) $t - z/\upsilon_{\mathrm{B}} < -T_{\mathrm{B}}$, (*ii*) $|t - z/\upsilon_{\mathrm{B}}| < T_{\mathrm{B}}$ and (*iii*) $t - z/\upsilon_{\mathrm{B}} > T_{\mathrm{B}}$ (see Supplementary Section 3 for more details). Hence, we require 3 different systems of PPEs connected by the corresponding boundary conditions. Each system of PPEs is composed by 2 different PPEs which account for the forward and backward propagation of $\mathbf{A}^{(E)}_{\omega_0}$ in the corresponding region of the problem. Furthermore, taking into account the all-dielectric nature of all regions, we can infer that $\mathbf{E}_{\omega_0}$ is completely uncoupled from $\mathbf{H}_{\omega_0}$ in the CAWEs and, consequently, $\mathbf{A}^{(H)}_{\omega_0}$ can be calculated from $\mathbf{A}^{(E)}_{\omega_0}$ by using Faraday's law working in ω-space.

The boundary conditions which connect the different regions are exclusively associated to a spatial scattering problem, provided that Δn_{eff} exhibits an invariant shape while propagates through the waveguide (otherwise, we would also observe a temporal scattering problem). Note that the moving temporal boundaries which define the modal perturbation $\Delta n_{\mathrm{eff}}(t - z/\upsilon_{\mathrm{B}})$ are actually spatial changes of n_{eff} which propagate through the z-axis. In this vein, we require to impose the spatial continuity of the tangential component of $\mathcal{E}$ and $\mathcal{H}$ at the moving spatial interfaces of the problem, which implies that the tangential component of $\mathbf{A}^{(E)}_{\omega_0}$ and $\mathbf{A}^{(H)}_{\omega_0}$ must be a continuous function at the interfaces that separate each region, i.e., at $|t - z/\upsilon_{\mathrm{B}}| = T_{\mathrm{B}}$. The combination of these boundary conditions and the PPEs will allow us to calculate the reflected and transmitted complex envelopes generated from the interaction of an incident pulse with the moving modal perturbation.

Specifically, the 2 PPEs associated to the forward and backward propagation of $\mathbf{A}^{(E)}_{\omega_0}(z,t) \simeq \mathcal{A}(z,t)\hat{u}_x$ in a given region is found to be (see Supplementary Section 3):

$$\left[\pm\partial_z + \left(\beta^{(1)} + \beta^{(1)}_{\mathrm{B}}\left(t - z/\upsilon_{\mathrm{B}}\right)\right)\partial_t - \mathrm{j}\frac{1}{2}\left(\beta^{(2)} + \beta^{(2)}_{\mathrm{B}}\left(t - z/\upsilon_{\mathrm{B}}\right)\right)\partial_t^2 + \mathrm{j}\beta^{(0)}_{\mathrm{B}}\left(t - z/\upsilon_{\mathrm{B}}\right)\right]\mathcal{A}(z,t) = 0, \quad (8)$$

with the sign "+" ("−") to describe the forward (backward) propagation. In Eq. (8), $\beta^{(1)}$ and $\beta^{(2)}$ are respectively the inverse of the group velocity and group-velocity dispersion coefficient of the fundamental mode, $\beta^{(0)}_{\mathrm{B}}$ and $\beta^{(1,2)}_{\mathrm{B}}$ are respectively the changes induced in $\beta^{(0)} = k_0 n_{\mathrm{eff}}(\omega_0)$ and $\beta^{(1,2)}$ by the modal perturbation, $k_0 = \omega_0/c_0$, and c_0 is the speed of light in vacuum. Each region of the problem is described by different $\beta^{(0,1,2)}_{\mathrm{B}}$ functions.

In the case that we can assume $\beta_{\mathrm{B}}^{(1,2)} \simeq 0$, Eq. (8) is reduced to Eq. (2) of [38], which leads to the pulse propagation equation of a temporal waveguide: two adjacent temporal index boundaries (allowed to move at a speed υ_{B}) defining a position-dependent temporal index window, which can carry optical pulses [39], [40]. A temporal waveguide can be created from extremely weak dynamic index perturbations ($\Delta n_{\mathrm{eff}} < 10^{-7}$), technologically feasible in silica waveguides, for instance, via traveling-wave electro-optic phase modulators or the cross-phase modulation effect [39].

2.4 White-Light Continuum Generation in Gases

For completeness, we will study the pulse propagation problem in an unguided medium. Concretely, as shown in Fig. 1(e), we will focus our attention on the propagation of an ultra-short pulsed paraxial wave (femtosecond regime) in an ionized gas (plasma) to perform white-light continuum (WLC) generation, an active research area in nonlinear optics [30], [41], [42]. WLC generation has attracted special attention as a means to achieve an ideal tunable ultrafast white-light laser source, a cornerstone in optics. In gases, the basic principle of WLC generation is based on the filamentation of ultra-short laser pulses, which emerges from a dynamic balance between Kerr-induced self-focusing and plasma-induced defocusing [43]. Thus, in this context, the comprehension of the propagation of ultra-short pulses is of fundamental importance. Remarkably, in this subsection, we will demonstrate that the GPPM can also be employed in such a scenario.

The basic idea is to consider the plasma as a weak homogeneous time-invariant medium perturbation. In this way, the phase constant of the optical medium can be described by an equivalent phase constant $\beta_{\mathrm{eq}}(\omega) = \beta(\omega) + \beta_{\mathrm{PL}}(\omega)$ accounting for the ideal phase constant β and the perturbation induced by the plasma β_{PL}. Hence, following this approach, the pulse propagation problem can be described using the GPPM (assuming a single optical carrier with angular frequency ω_0) by 1 PPE accounting for the forward propagation of $\mathbf{A}_{\omega_0}^{(E)}(\mathbf{r}, t) = \mathcal{A}(\mathbf{r}, t)\hat{u}_x$ along the z-axis (see Supplementary Section 5):

$$\mathrm{j}\left[\frac{\mathrm{j}}{2\beta^{(0)}}\Delta_{\mathrm{T}} + \partial_z + \hat{\mathrm{D}} + \frac{1}{2}\hat{\alpha}\right]\mathcal{A}(\mathbf{r}, t) = \beta_{\mathrm{PL}}^{(0)}\mathcal{A}(\mathbf{r}, t) - \mathrm{j}\hat{\mathrm{D}}_{\mathrm{PL}}\mathcal{A}(\mathbf{r}, t) + \hat{\mathrm{q}}_{\mathrm{I}}\left[|\mathcal{A}(\mathbf{r}, t)|^2\mathcal{A}(\mathbf{r}, t)\right] + \hat{\mathrm{q}}_{\mathrm{R}}\left[\left(f(t) * |\mathcal{A}(\mathbf{r}, t)|^2\right)\mathcal{A}(\mathbf{r}, t)\right], \tag{9}$$

where $\beta^{(0)} := \beta(\omega_0)$, $\beta_{\mathrm{PL}}^{(0)} := \beta_{\mathrm{PL}}(\omega_0)$, $\Delta_{\mathrm{T}} := \partial_x^2 + \partial_y^2$ is the transverse Laplacian operator, $\hat{\mathrm{D}}$ is the dispersion operator of the medium in absence of plasma which describes the frequency dependence of β, $\hat{\mathrm{D}}_{\mathrm{PL}}$ is the dispersion operator of the plasma associated to the frequency dependence of β_{PL}, and $\hat{\mathrm{q}}_{\mathrm{I}}$ and $\hat{\mathrm{q}}_{\mathrm{R}}$ are linear operators accounting for the optical dispersion induced by the third-order nonlinear effects related to the electronic ($\hat{\mathrm{q}}_{\mathrm{I}}$) and nuclear ($\hat{\mathrm{q}}_{\mathrm{R}}$) motions of atoms when an incident electromagnetic field stimulates the medium. It should be noted that we do not require to impose boundary conditions to the above PPE given that we have assumed a homogeneous time-invariant medium perturbation. Accordingly, the PPE applies in a unique spatio-temporal region $(z, t) \in [0, L] \times \bar{\mathbb{R}}$. Finally, it is worthy to highlight that Eq. (9) can also be used to describe the propagation of pulses in gas-filled waveguides [44] by omitting the term $\mathrm{j}\Delta_{\mathrm{T}}/(2\beta^{(0)})$, which accounts for the pulse diffraction.

3. Conclusion

Overall, the GPPM generalizes the formalism describing the propagation of pulses in any kind of single-core and multi-core optical fiber taking into account the spatial and temporal medium perturbations along with higher-order nonlinear effects and, consequently, leading to the emergence of a new fiber design toolbox. As a result, a large diversity of fiber-optic applications can be covered by the GPPM, spanning not only the next-generation optical communications based on space-division multiplexing transmissions [45], but also biomedical [46], [47] and physical applications [3],

[47], [48]. Likewise, the GPPM can also be applied to non-circular waveguides (e.g., rectangular waveguides) and unguided media, widening the scope of our results to integrated and free-space photonics. Outstandingly, the GPPM could be of great utility to analyze the pulse dispersion induced by waveguide perturbations (e.g., bends) in integrated photonics, which may appear when the waveguide is incorporated in ultra-compact optical devices [49], [50].

The potential of the GPPM will be further investigated in future works by performing numerical simulations of the different scenarios analyzed herein. A cost-efficient numerical computation of the GPPM can be guaranteed in perturbed and unperturbed media by using the local split-step Fourier method reported in [23], which requires a detailed revision to include the necessary boundary conditions that connect the different systems of PPEs inferred from the GPPM. In particular, this will be of capital importance in light-scattered systems.

References

[1] J. C. Maxwell, "A dynamical theory of the electromagnetic field," *Phil. Trans. Roy. Soc. Lond.*, vol. 155, pp. 459–512, Jan. 1865.
[2] N. S. Kapany, *Fiber Optics. Principles and Applications*. New York, NY, USA: Academic Press, 1967.
[3] T. G. Philbin, C. Kuklewicz, S. Robertson, S. Hill, F. König, and U. Leonhardt, "Fiber-optical analog of the event horizon," *Science*, vol. 319, no. 5868, pp. 1367–1370, Mar. 2008.
[4] D. V. Churkin *et al.*, "Recent advances in fundamentals and applications of random fiber lasers," *Adv. Opt. Photon.*, vol. 7, no. 3, pp. 516–569, Aug. 2015.
[5] J. E. Antonia-López, Z. S. Eznaveh, P. L. LiKamWa, A. Schülzgen, and R. Amezcua-Correa, "Multicore fiber sensor for high-temperature applications up to 1000 °C," *Opt. Lett.*, vol. 39, no. 15, pp. 4309–4312, Aug. 2014.
[6] S. Karbasi, R. J. Frazier, K. W. Koch, T. Hawkins, J. Ballato, and A. Mafi, "Image transport through a disordered optical fibre mediated by transverse Anderson localization," *Nature Commun.*, vol. 5, Feb. 2014, Art. no. 3362.
[7] Q. Wang, G. Rajan, P. Wang, and G. Farrell, "Polarization dependence of bend loss for a standard single mode fiber," *Opt. Exp.*, vol. 15, no. 8, pp. 4909–4920, Apr. 2007.
[8] P. Russell, "Photonic crystal fibers," *Science*, vol. 299, no. 5605, pp. 358–362, Jan. 2003.
[9] V. Ramaswamy, W. G. French, and R. D. Standley, "Polarization characteristics of noncircular core single-mode fibers," *Appl. Opt.*, vol. 17, no. 18, pp. 3014–3017, Sep. 1978.
[10] M. Takahashi, R. Sugizaki, J. Hiroishi, M. Tadakuma, Y. Taniguchi, and T. Yagi, "Low-loss and low-dispersion-slope highly nonlinear fibers," *J. Lightw. Technol.*, vol. 23, no. 11, pp. 3615–3624, Nov. 2005.
[11] T. Hayashi, T. Taru, O. Shimakawa, T. Sasaki, and E. Sasaoka, "Design and fabrication of ultra-low crosstalk and low-loss multi-core fiber," *Opt. Exp.*, vol. 19, no. 17, pp. 16576–16592, Aug. 2011.
[12] I. P. Kaminow, T. Li, and A. E. Willner, *Optical Fiber Telecommunications VIA: Components and Subsystems*. Oxford, UK: Elsevier, 2013, ch. 8.
[13] A. Taflove and S. C. Hagness, *Computational Electrodynamics: The Finite-Difference Time-Domain Method*. Boston, MA, USA: Artech House, 2005.
[14] G. Sztefka and H.-P. Nolting, "Bidirectional eigenmode propagation for large refractive index steps," *IEEE Photon. Technol. Lett.*, vol. 5, no. 5, pp. 554–557, May 1993.
[15] G. V. Eleftheriades, A. S. Omar, L. P. B. Katehi, and G. M. Rebeiz, "Some important properties of waveguide junction generalized scattering matrices in the context of the mode matching technique," *IEEE Trans. Microw. Theory Techn.*, vol. 42, no. 10, pp. 1896–1903, Oct. 1994.
[16] B. Maes, P. Bienstman, and R. Baets, "Modeling of Kerr nonlinear photonic components with mode expansion," *Opt. Quantum Electron.*, vol. 36, no. 1–3, pp. 15–24, Jan. 2004.
[17] M. Kolesik, *Computational Optics: Beam Propagation Methods*. Hauppauge, NY, USA: Nova Science Publishers, 2017.
[18] G. L. Pedrola, *Beam Propagation Method for Design of Optical Waveguide Devices*. New York, NY, USA: John Wiley & Sons, 2015.
[19] P. V. Mamyshev and S. V. Chernikov, "Ultrashort-pulse propagation in optical fibers," *Opt. Lett.*, vol. 15, no. 19, pp. 1076–1078, Oct. 1990.
[20] F. Poletti and P. Horak, "Description of ultrashort pulse propagation in multimode optical fibers," *J. Opt. Soc. Amer. B.*, vol. 25, no. 10, pp. 1645–1654, Oct. 2008.
[21] A. Mecozzi, C. Antonelli, and M. Shtaif, "Coupled Manakov equations in multimode fibers with strongly coupled groups of modes," *Opt. Exp.*, vol. 20, no. 21, pp. 23436–23441, Sep. 2012.
[22] S. Mumtaz, R. J. Essiambre, and G. P. Agrawal, "Nonlinear propagation in multimode and multicore fibers: Generalization of the Manakov equations," *J. Lightw. Technol.*, vol. 31, no. 3, pp. 398–406, Feb. 2013.
[23] A. Macho, C. García-Meca, F. J. Fraile-Peláez, F. Cortés-Juan, and R. Llorente, "Ultra-short pulse propagation model for multi-core fibers based on local modes," *Scientific Reports*, vol. 7, Nov. 2017, Art. no. 16457.
[24] Y. Sivan, S. Rozenberg, and A. Halstuch, "Coupled-mode theory for electromagnetic pulse propagation in dispersive media undergoing a spatiotemporal perturbation: Exact derivation, numerical validation, and peculiar wave mixing," *Physical Rev. B*, vol. 93, Apr. 2016, Art. no. 144303.
[25] D. Gloge, "Weakly guiding fibers," *Appl. Opt.*, vol. 10, no. 10, pp. 2252–2258, Oct. 1971.
[26] T. Hayashi, T. Sasaki, E. Sasaoka, K. Saitoh, and M. Koshiba, "Physical interpretation of intercore crosstalk in multicore fiber: Effects of macrobend, structure fluctuation, and microbend," *Opt. Exp.*, vol. 21, no. 5, pp. 5401–5412, Feb. 2013.

[27] M. Morant, A. Macho, and R. Llorente, "On the suitability of multicore fiber for LTE-advanced MIMO optical fronthaul systems," *J. Lightw. Technol.*, vol 34, no. 2, pp. 676–682, Jan. 2016.
[28] A. Macho, M. Morant, and R. Llorente, "Next-generation optical fronthaul systems using multicore fiber media," *J. Lightw. Technol.*, vol. 34, no. 20, pp. 4819–4827, Oct. 2016.
[29] A. Macho, C. García-Meca, F. J. F.-Peláez, M. Morant, and R. Llorente, "Birefringence effects in multi-core fiber: Coupled local-mode theory," *Opt. Exp.*, vol. 24, no. 19, pp. 21415–21434, Sep. 2016.
[30] N. Múnera, "Optimization of broadband white light continuum in gases for Z-scan and other nonlinear applications," Ph.D. dissertation, CREOL, Univ. Central Florida, Orlando, Florida, EEUU, 2018.
[31] B. E. A. Saleh and M. C. Teich, *Fundamentals of Photonics*. New York, NY, USA: Wiley, 2007, chs. 6 and 22.
[32] W.-P. Huang, "Coupled-mode theory for optical waveguides: An overview," *J. Opt. Soc. Am.*, vol. 11, no. 3, pp. 963–983, Mar. 1994.
[33] J. T. Mendonça and P. K. Shukla, "Time refraction and time reflection: Two basic concepts," *Physica Scripta*, vol. 65, no. 2, pp. 160–163, Mar. 2002.
[34] A. M. Prokhorov, G. A. Smolenski, and A. N. Ageev, "Optical phenomena in thin-film magnetic waveguides and their technical application," *Soviet Phys. Uspekhi*, vol. 27, no. 5, pp. 339–362, May 1984.
[35] H. Otmani *et al.*, "Simulation of magneto-optical properties of magnetic photonic crystal waveguides," *J. Nanophotonics*, vol. 13, no. 2, pp. 0260021–0260027, Apr. 2019.
[36] A. M. Weiner, *Ultrafast Optics*. Hoboken, NJ, USA: John Wiley & Sons, 2009, ch. 6.
[37] B. W. Plansinis, W. R. Donaldson, and G. P. Agrawal, "Cross-phase-modulation-induced temporal reflection and waveguiding of optical pulses," *J. Opt. Soc. Amer. B*, vol. 35, no. 2, pp. 436–445, Feb. 2018.
[38] B. W. Plansinis, W. R. Donaldson, and G. P. Agrawal, "What is the temporal analog of reflection and refraction of optical beams?," *Physical Rev. Lett.*, vol. 115, no. 183901, pp. 1–5, Oct. 2015.
[39] B. W. Plansinis, W. R. Donaldson, and G. P. Agrawal, "Temporal waveguides for optical pulses," *J. Opt. Soc. Amer. B*, vol. 33, no. 6, pp. 1112–1119, Jun. 2016.
[40] J. Zhou, G. Zheng, and J. Wu, "Comprehensive study on the concept of temporal optical waveguides," *Physical Rev. A*, vol. 93, no. 063847, pp. 1–5, Jun. 2016.
[41] P. B. Corkum, C. Rolland, and T. Srinivasan-Rao, "Supercontinuum generation in gases," *Physical Rev. Let.*, vol. 57, no. 18, pp. 2268–2271, Nov. 1986.
[42] R. R. Alfano, *The Supercontinuum Laser Source. The Ultimate White Light*. New York, NY, USA: Springer, 2016, ch. 7.
[43] P. Béjot *et al.*, "Higher-order Kerr terms allow ionization-free filamentation in gases," *Physical Rev. Lett.*, vol. 104, no. 103903, pp. 1–4, Mar. 2010.
[44] R. Sollapur *et al.*, "Resonance-enhanced multi-octave supercontinuum generation in antiresonant hollow-core fibers," *Light: Sci. Appl.*, vol. 6, p. e17124, Dec. 2017.
[45] P. J. Winzer, D. T. Neilson, and A. R. Chraplyvy, "Fiber-optic transmission and networking: The previous 20 and the next 20 years," *Opt. Exp.*, vol. 26, no. 18, pp. 24190–24239, Sep. 2018.
[46] E. R. Andresen, S. Sivankutty, V. Tsvirkun, G. Bouwmans, and H. Rigneault, "Ultrathin endoscopes based on multicore fibers and adaptive optics: A status review and perspectives," *J. Biomed. Opt.*, vol. 21, no. 12, Oct. 2016, Art. no. 121506.
[47] X. Lu *et al.*, "Ultrasensitive, high-dynamic-range and broadband strain sensing by time-of-flight detection with femtosecond-laser frequency combs," *Scientific Reports*, vol. 7, Oct. 2017, Art. no. 13305.
[48] N. Jovanovic, O. Guyon, H. Kawahara, and T. Kotani, "Application of multicore optical fibers in astronomy," in *Proc. Opt. Fiber Commun. Conf. Exhib.*, 2017, paper W3H.3.
[49] D. Marpaung, J. Yao, and J. Capmany, "Integrated microwave photonics," *Nature Photon.*, vol. 13, pp. 80–90, Jan. 2019.
[50] C. García-Meca, A. Macho, and R. Llorente, "Optical supersymmetry in the time domain," *arXiv:1903.12639*, Mar. 2019.